JOURNAL OF Applied Polymer SCIENCE

Influence of Compatibilizer Content on PA/NBR Blends Properties: Unusual Characterization and Evaluation Methods

A. C. O. Gomes,[1] B. G. Soares,[2] M. G. Oliveira,[3] L. A. Pessan,[1] C. M. Paranhos[4]

[1]Materials Engineering Department, Federal University of São Carlos, São Carlos, Sao Paulo, Brazil
[2]Institute of Macromolecules Professor Eloisa Mano, Federal University of Rio de Janeiro, Rio de Janeiro, Brazil
[3]Materials Characterization and Processing Department, National Institute of Technology, Rio de Janeiro, Brazil
[4]Chemistry Department, Federal University of São Carlos, São Carlos, Sao Paulo, Brazil

Correspondence to: A. C. O. Gomes (E-mail: acogomes@gmail.com)

ABSTRACT: NBR/PA6 blends were prepared at the melt state and with the use of masterbatches. Compatibilization with NBR-oxazoline was tested with the aim of enhancing the blend performance and to obtain more appropriated morphology. The effect of compatibilizer content was studied through the characterization of blend mechanical properties, creep behavior, swelling, PA6 phase crystallinity, morphology, and rheological properties, including pressure-volume-temperature behavior. The results show a more significant elastomeric behavior for blends with 5 and 7 phr of compatibilizer, with deleterious effects for higher content. The migration of compatibilizer into elastomeric phase was documented by electronic microscopy, and corroborated by an increase in free volume of the samples. © 2012 Wiley Periodicals, Inc. J. Appl. Polym. Sci. 000: 000–000, 2012

KEYWORDS: PA; NBR; compatibilization; rheology; PVT; creep; morphology

Received 30 June 2010; accepted 26 March 2012; published online
DOI: 10.1002/app.37792

INTRODUCTION

Thermoplastic elastomer vulcanizates (TPV), in overall, are biphasic materials with mechanical properties like an elastomer, and processing characteristic like a thermoplastic. This kind of material can yet generate new properties due synergistic effects practically unforeseeable. TPVs obtained by polymer blend/dynamic vulcanization is nowadays the most common way to develop new materials with greater applicability potential, due to the several possibilities of polymer combinations.[1,2] The field of applicability is broad, embracing since common every-day tool to automotive parts and engineering materials.

The morphology development of a TPV is quite different of common polymeric blends, because the increasing viscosity of the elastomeric phase due its vulcanization process. It have been cited in the literature that the increase of viscosity of elastomeric phase generates a increase in shear tension, leading to a better breaking particles process and resulting in a better morphology.[3,4] Karger-Kocsis[5] comments that this is a very simplest scenario that does not take in account important facts as the heat generated by crosslinking reaction, crosslinking rate, thermal degradation etc. Yet, the viscosity increasing of elastomeric phase would increase the viscosity difference between blend components, what would make more difficult the particles breaking. However, some authors showed that, for some systems, the interfacial tension or polarity match was more effective on the morphological development of the polymer blends than the viscosity ratio of the polymers.[6] The subject is still far from a converging point of view.

The development of a better morphology is frequently attempted by the compatibilization of the blend. An agent is considered a compatibilizer when its presence in interface decreases the interfacial tension between phases, generating smaller dispersed particles into the blend matrix. Beyond that, the presence of these molecules of compatibilizer in the surface of the particle can avoid coalescence process during processing. The improvement of the blend morphology, i.e., a finer size and distribution of the disperse domain, commonly is reflected to better mechanical properties. If the interaction between phases generated by the compatibilizer is strong enough to increase the interfacial adhesion, this could also improve the mechanical properties of the blend.[7,8]

The blend of polyamide 6 (PA6) and acrylonitrile-butadiene copolymer rubber (NBR) may generate a material with good hot oil resistance and good mechanical properties, mainly at high temperatures.[9] Despite of the potential, few works have been

published in the last years with this blend, probably due to thermal and processing barriers. The high temperature needed to process and mold PA6 causes elastomer degradation.

Blends of PA and NBR are presented in the literature into a wide range of applications. The most cited are NBR composites with polyamide fibres,[10] and tenacification of a PA matrix by incorporation of low content of NBR.[11–13]

The PA/NBR blends TPVs have its beginning in a sequence of works of Coran and Patel[14] about various thermoplastic elastomers and its processing characteristics. Mehrabzadeh and Delfan [15] began their research with tenacification of PA11 with NBR, tried the dynamic vulcanization of a blend (1996) and changed to PA6/NBR TPV from year 2000. In 2008, TPV's of PA, polypropylene, NBR and chlorobutylic elastomer are studied by Van Dyke et al.[16] Among all strategies taken to obtain a technological useful material based in PA/NBR, some ones may be pointed out. The first one is the substitution of NBR by modified versions, as carboxylated NBR[17,18] and hydrogenated NBR.[19,20] Despite the good results, this strategy is not considered to our objectives, once these materials are more expensive and less elastomerics than neat NBR. The second strategy is the substitution of PA by a copolymer with lower fusion temperature, what would save the elastomer from thermal degradation due processing.[21–23] This strategy, however, is incoherent to one of the most important objectives to combine PA and NBR, what would be the possibility of high temperatures applications.

The attempt of minimizing the problems with blend processing in previous work showed a successful strategy in incorporating additives by the use of a masterbatch (MB) system. The improvements, however, was not reflected by the blend morphology, that presented the elastomer as blend matrix.[24] Part of problem was solved by the study of processing conditions, but a coarse morphology was still obtained.

The use of oxazoline-modified NBR (NBR-oxa) as a compatibilizer was considered to modify the blend behavior as a whole, and to reach a better morphology. This strategy is widely described in the literature as an efficient compatibilization system for blends with amine or carboxyl-end polymers, as polyamides.[25]

The objective of this work was to evaluate the effect of the compatibilizer content on the final properties of the blend PA6/NBR, including mechanical and rheological properties. The results reported here show the advantages of developing a new TPV material, dimensionally stable and with possible application at more severe conditions than most similar materials available in the market.

EXPERIMENTAL

Materials

NBR (28% wt/wt of acrylonitrile; Mooney viscosity = 60, at 100°C) and phenolic resin SP1045 (PR) were kindly supplied by Petroflex Ind. e Com. PA6 (MFI = 19.6 g/10 min, density 1.14 g/cm^3) was kindly supplied by Radici Group. Copolymer of ethylene-vinyl acetate modified with maleic anhydride (EVAMA—28% of vinyl acetate, 0.8% wt/wt of maleic anhydride, MFI = 16 g/10 min, density 0.95 g/cm^3) was obtained commercially from Proquimil. The antioxidant Naugard 445® was kindly supplied by Crompton Corporation of Brazil. The antioxidants Irganox 1010® and Irgafos 168® was obtained from Ciba Corporation do Brazil. Stannous chloride ($SnCl_2$) was obtained commercially from VETEC of Brazil. All commercial products were used as received. NBR-oxa (oxazoline content ~ 3 mmol/g) was prepared in our laboratory by chemical modification of NBR, as described by Almeida et al.[26]

Table I. Blends Compositions, Contents in phr (Parts Per Hundred of Resin)

			Added during blending	
Sample	MBPA6	MBNBR	NBR-oxa	Others additives
Czero	PA6 + EVAMA (5) + Irganox 1010 (2.5) + Irgafos 168 (2.5)	NBR + Naugard 445 (7.5)	-	RF + $SnCl_2$ (10 : 0.5) Naugard 445 (2.5)
C2			2	
C5			5	
C7			7	
C10			10	

Sample Preparation

Blend Preparation. All samples were prepared in an internal chamber mixer coupled with a torque rheometer Brabender Plastograph, with bambury rotors at 60 rpm of speed. The MB of PA6 and 5 phr of EVAMA (MBPA) was prepared at 240°C, and the MB of NBR and antioxidants (MBNBR), at 40°C, both processed during 3 min. All blends were obtained by 50 : 50 combinations of MBs (in phr), at 220°C, during 9 min. The blend compositions are described in Table I. All samples were dried in vacuum oven at 100°C before each processing step. The components were added in the following order: pre-heated MBPA (1 min), MBNBR (2 min), NBR-oxa (2 min), phenolic resin and stannous chloride as crosslinking system (2 min), and Naugard (added in the last minute of blending).

As described in Gomes et al.,[24] each additive has an important role in the morphology development, as well as in the final properties of the blend. The EVAMA in the MBPA is present to increase phase viscosity and improve the blending mechanism. Its presence can also contribute to increase the compatibility with the elastomeric phase. This effect, however, could not be proved based on previous results. The antioxidant mixture and contents in the MBNBR and MBs blend were carefully studied in terms of thermal resistance and influence in final properties, and this work may be published soon. The system based in phenolic resin and stannous chloride for the dynamic crosslinking of NBR phase is well known in the literature, as well as the oxazoline-modified NBR as compatibilizer agent.[24]

Phase Selective Extraction and Swelling in Methyl-Ethyl Ketone

Samples were cut from a sheet, in approximately 10 mm × 10 mm × 2 mm. Samples pieces were extracted in Soxhlet system,

Table II. Results of Tensile Strength, Selective Extraction (Acetic Acid for PA Phase, and Toluene for No Crosslinked NBR Phase) and Swelling in Methyl-Ethyl ketone (MEK—Good Affinity to NBR Phase)

	σ (±1.0 MPa)	ε (±30%)	E (±60 MPa)	Extraction residue (±3%)		Swelling in MEK (±3%)
				Acetic acid	Toluene	
Czero	10.4	120	131	40	80	58
C2phr	8.8	57	149	58	92	44
C5phr	10.1	117	169	43	87	42
C7phr	9.8	109	148	51	93	32
C10phr	11.4	134	145	34	89	24

σ = stress at break; ε = elongation at break; E = Young modulus.

with toluene (NBR phase) or acetic acid (PA6 phase), during 24 h, then dried in vacuum oven. The acetic acid was chonsen due its extraction capacity, low toxicity, cost and reuse possibility. The time of extraction was defined by a control sample, composed just by one of the phases of the blend (that to be extracted). In 24 h, all the control sample mass was extract by its selective solvent. The swelling tests proceeds with the samples immersed in methyl-ethyl ketone (MEK) during a week, and the swelling was described in terms of mass gain.

Thermal Analysis

Isothermal differential calorimetry was performed in a Perkin–Elmer DSC 7, under nitrogen flux, at 200°C. The crystallinity degree was calculated from the rate $\Delta H_m/\Delta H_m^o$, where $\Delta H_m^o = 240$ J/g.[27] The Avrami parameters were calculated following the equation:

$$\ln\left[1 - \ln(1 - \chi(t))\right] = \ln k + n \ln t$$

where $\chi(t)$ is the crystallized fraction of polymer until time t, n is related to the crystallite form and k is the crystallization rate. The beginning of crystallization curve is adjusted to a linear regression and the parameters are obtained from the equation logarithm form.[27]

FTIR Spectroscopy

Fourier transformed infrared (FTIR) spectra were obtained in a Varian 3100 Excalibur, between 4000 cm^{-1} and 600 cm^{-1}.

Tensile Stress

Samples were injected in a Battenfeld Plus 35, with 110 bar of mold pressure, 240°C of injection temperature and 80 bar of injection pressure, following DIN53504 standards. The test was performed in a universal testing machine EMIC DL-2000, at speed of 200 mm/min.

Creep Test

Samples were cut from pressed sheets of approximately 0.1 mm of thickness, in dimensions of approximately 6 mm × 30 mm. The test was realized in DMA Q800, of TA Instruments, in film tension clamp, at 25°C, with tension of 0.1 MPa, tension time of 30 min, recover time of 60 min.

Pressure-Volume-Temperature (PVT) Behavior and Specific Volume Measurement

Pressure–volume–temperature behavior was investigated in a Ceast Smart Rheo 2000 rheometer. A known mass of milled sample was loaded to the cylinder contender, the bottom of the capillar was sealed with a metal plug and pressure was applied through a piston with a PTFE disc seal. Specific volume measurements were carried out in each pressure and temperature, in a 20–60 MPa pressure range and 250–230°C temperature range.

Capillary Rheometry and Extrudate Swell

Milled samples were tested at 250°C, in shear rate range of 10–800 s^{-1} in a Ceast Smart Rheo 2000 rheometer. The diameter of extruded filament was measured after test, with Mitutoyo digital caliper rule, and the swelling was calculated from the ratio of diameters.

Scanning Electronic Microscopy

The analysis was performed on FEG XL30 Philips equipment. The samples were cryogenically fractured and chemical stained by osmium tetroxide (OsO_4), to selectively stain the unsaturated phase. The samples were then coated with carbon and analyzed with a backscattered electron detector. The stained phase (NBR phase) appears as the "brighter" one. The domain size distribution was obtained through the free software ImageJ 1.42q, from NIH (http://rsb.info.nih.gov/ij).

RESULTS AND DISCUSSION

Tensile Stress

Table II presents the results of tensile stress for all samples. There is no significant difference among samples with different contents of compatibilizer. This indicates that the compatibilization does not result in changes of morphology or interaction between phases strong enough to modify a macroscopic property as tensile strength. It is important to emphasize that the analysis conditions are very exigent to a material where the matrix is a thermoplastic. The elongation speed used was 200 mm/min, which is a typical condition for testing elastomeric samples. The velocity chosen showed itself too drastic for a TPV material, which response, in this case, was not capable to reflect differences in interphase interactions.

FTIR Analysis

The confirmation of the compatibilization process was obtained by FTIR analysis. The FTIR spectra were obtained before and after selective extraction in acetic acid, which is selective for polyamide phase. The objective was to distinguish, in the insoluble fraction of the selective extraction, those peaks derived from "*in situ*" reaction due to the compatibilization process. It is believed that a

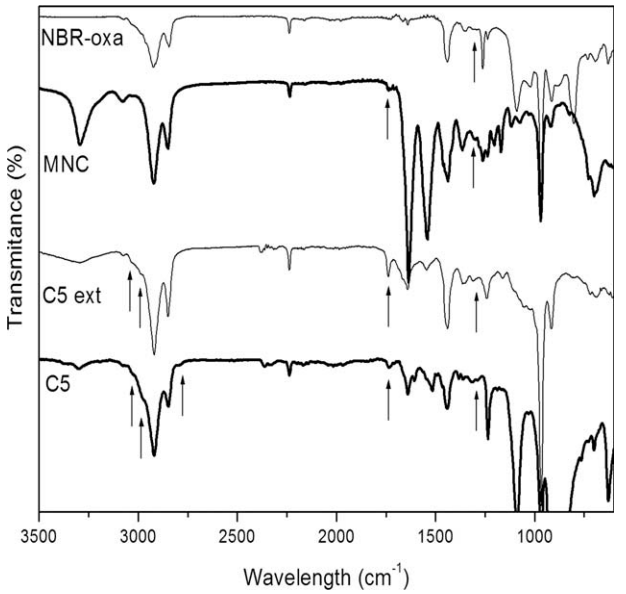

Figure 1. Comparative FTIR spectra of NBR-oxazoline and Czero sample, and C5 sample before and after extraction (C5 ext).

reaction between carboxyl group of PA6 and the oxazoline group of modified NBR occurs and generates an ester-imide linkage.[28] The peaks obtained were related to ester and amides, slightly dislocated to smaller values of energy, due the neighborhood with the two functional groups. Jeziórska[28] reported peaks at 1100 cm^{-1} and 1019 cm^{-1} for new amide groups generated. In Figure 1, it can be noticed the presence of new bands comparing with the non-compatibilized sample (Czero). Absorption bands around 3000 cm^{-1} can be associated to new stretching of —CH_2- groups, located between ester and amide or amide and amine groups (depending of which polyamide terminal group did react) of the compatibilizer formed "*in situ*." The peak located in 1360 cm^{-1} also can be associated to these alkyl groups.[29] A band in 1730 cm^{-1} is frequently associated to the carbonyl group of ester, present in the new macromolecule.[28] This band becomes more intense in the extracted sample. If the compatibilizer formed "*in situ*" is insoluble in acetic acid, it is expected that this band increases its intensity in the residue of extraction.

Selective Extraction and Swelling

The first observation with selective extraction is reached from visual aspect of samples after extraction. When the PA phase is selective extracted, the sample defined form is destroyed, resting a "powder like" material, while non-compatibilized samples remain as a whole. This phenomenon indicates that the NBR phase is present as dispersed phase in compatibilized blends.

The results for selective extraction residues show better extraction of PA6 phase (in acetic acid) in the sample with 2 phr of compatibilizer, and the residue becomes higher with the increase of compatibilizer content. This result is an indicative that the morphology of the samples is affected only from 5 phr of compatibilizer. The extraction in toluene (selective for not-crosslinked NBR phase) suggests that the compatibilizer has an important role in the crosslinking efficiency. The presence of compatibilizer leads to a higher residue content in toluene, indicating higher crosslinking of elastomer phase. The swelling results in MEK indicate that the higher content of compatibilizer, the smaller volume of solvent absorbed by the NBR phase. This result also suggests the NBR dispersed/PA6 matrix morphology. The decrease of swelling suggests higher restriction of NBR into the thermoplastic matrix; in other words, better fixation of the disperse domains and interface with the matrix, as well as the higher degree of crosslinking of NBR phase.

Thermal Analysis

Table III shows crystallinity degree (X_c), crystallization time for 50% of the crystallizable fraction of polymer ($t_{1/2}$) and Avrami parameters (k e n) related to the crystallization of PA6. The total crystallinity degree of samples decreases with the presence of compatibilizer. As compatibilizer content increases, $t_{1/2}$ values increase, indicating that the compatibilization is damaging the crystallization process of the semicrystalline phase. This hypothesis is consistent with the idea that the compatibilization increases the interface between components, increasing the interaction between molecules and disordering the molecules organization.

The crystallization rate (k) decreases with the presence and increasing content of compatibilizer. The variation of n values indicates a slight influence of the presence of compatibilizer in the morphological characteristics of PA6 crystallites.

Creep Behavior

The creep test is an important mechanical test due to the good correlation to deformations that may occur in the final applications of materials.[30,31]

The creep behavior is closely related to physical ageing, i.e., damages caused by slow structural relaxation of polymeric

Table III. Values of Crystallinity Degree (X_c), Time of Crystallization ($t_{1/2}$), Avrami Parameters (k—Crystallization Rate and n—Morphological Factor) and Die Swell of Samples With Different Contents of Compatibilizer

	$t_{1/2}$ (±0.1 min)	X_c (±1%)	k (± 1.10^{-4} s^{-1})	n (±0.4)	Die swell (±3%)
Czero	3.2	36	3.8	2.2	81
C2phr	3.7	21	2.1	3.0	72
C5phr	3.9	26	1.9	2.4	63
C7phr	4.1	19	1.9	2.3	63
C10phr	4.4	18	1.7	2.2	96

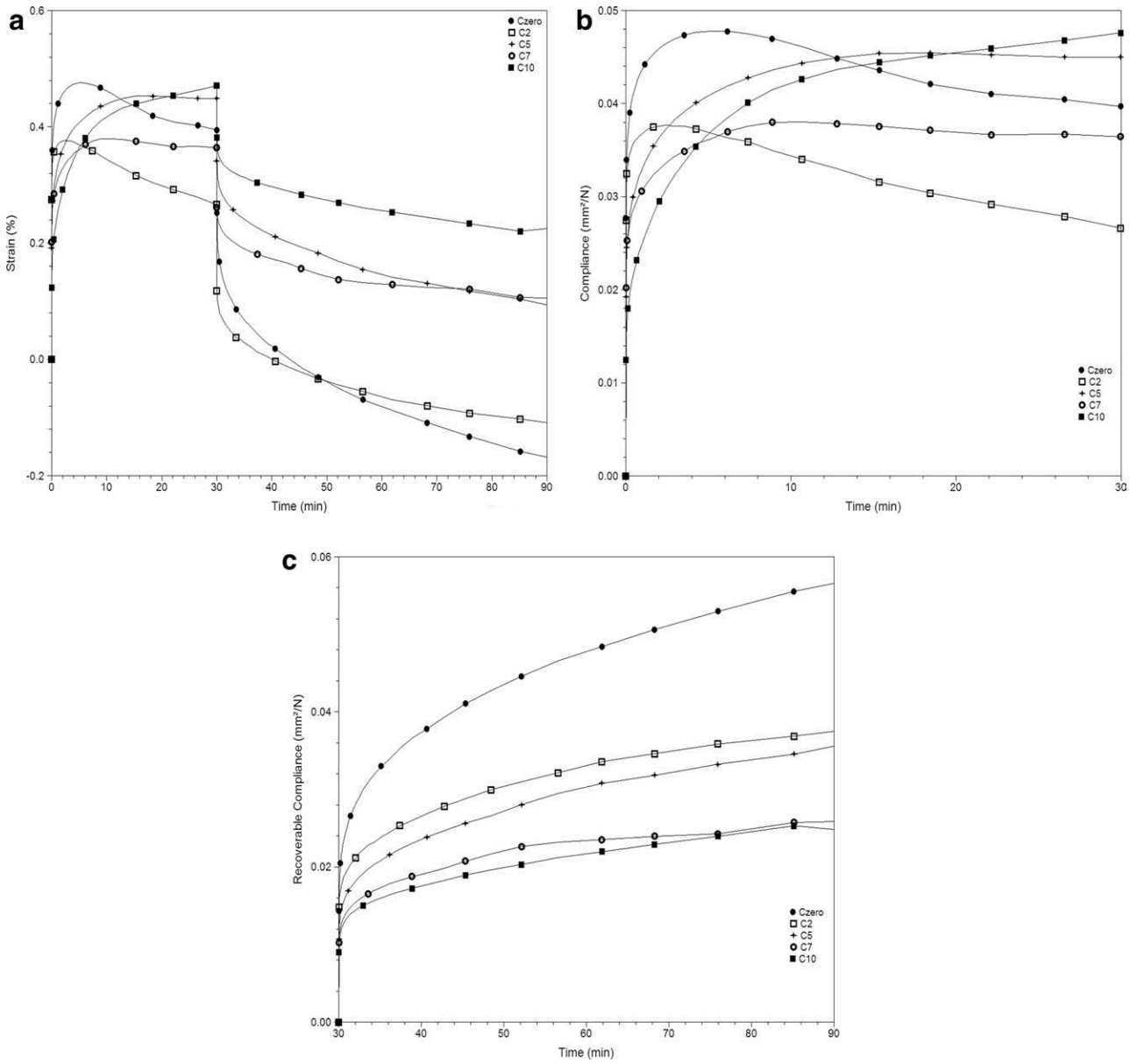

Figure 2. Creep behavior of all samples, being (a) strain curves, (b) creep compliance curves, and (c) recoverable compliance curves.

chains.[32] Therefore, the creep test can provide important information about how the compatibilization process is acting on the interphase, and as efficient the copolymer generated "*in situ*" acts in the linkage between phases and its stabilization. The creep tests show the best profile of deformation/recover in samples with 5 and 10 phr of compatibilizer [Figure 2(a)]. The "negative deformation" occurs due to relaxation phenomena of the pressed sample, as extensively discussed in previous work.[33] C5 is the only sample which stabilizes the strain into test time interval, indicating its superior stability. The creep compliance is smaller for C2 [Figure 2(b)] and the best recoverable compliance is obtained by Czero sample [Figure 2(c)]. This behavior can be explained by the compatibilization effect in the sample morphology. The decrease of elastomeric domains into the rigid matrix leads to a decrease in sample modulus.[33] The test shows C5 as the best sample, due to its stability and higher recovery capacity.

PVT Behavior

The description of rheological behavior of polymeric blends depends on, in majority of the cases, corrections relative to interactions among blend components. The specific volume of a material as a function of temperature and pressure is described by the called state equations, or pressure-volume-temperature (PVT) relationship, and is also an important factor for the understanding of polymeric blends rheology.[32] Once interaction parameters are applied in equations of PVT behavior, we can obtain interesting information about the interactions created by the compatibilization process, directly from PVT data. In addition, Fernández et al.[34,35] successfully determined numeric

Applied Polymer SCIENCE

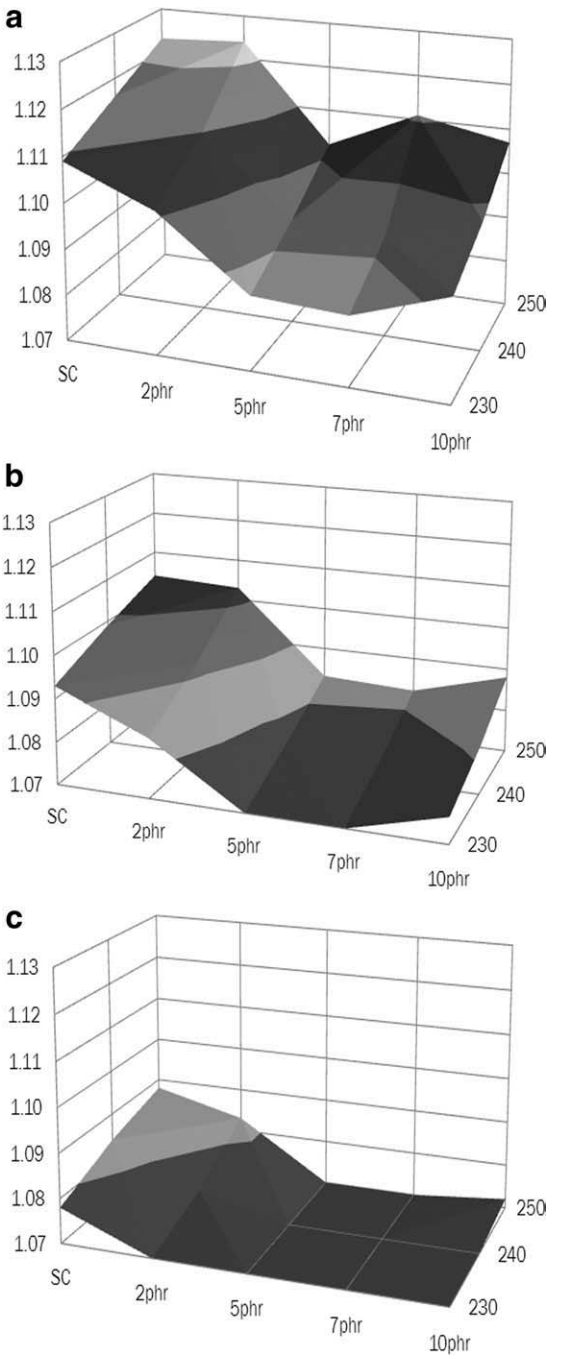

Figure 3. Specific volume variations with temperature and pressures (*x* axis—compatibilization content [phr]; *y* axis—temperature [°C]; *z* axis—specific volume [cm^3/g]), being the gray gradient relative to different specific volume ranges. Pressures: (a) 20 MPa, (b) 40 MPa, and (c) 60 MPa.

values to the fractional free volume fraction of glassy polymers as a function of temperature, using a combination of theoretical equations and PVT results. From their discussions, is reasonable to consider the analysis of specific volume at different temperatures and pressures as a tacit discussion about free volume.

The Figure 3 shows the variation of specific volume with the content of compatibilizer. The specific volume varies considerably, and the difference increases with the decreasing of temperature. This effect can be explained by the influence of temperature in molecular mobility. A lower temperature leads to a better accommodation in more stable and organized superstructures, decreasing differences due to chemical interactions.

The sample with 2 phr of compatibilizer begins to differ from Czero sample only over 40 MPa of pressure. Samples with 5 and 7 phr are very similar, except with 20 MPa of pressure at 250°C, where C7 shows higher specific volume. The decreasing of temperature to 230°C equalizes the behavior of C5 and C7 samples.

It is important to notice that 10 phr of compatibilizer leads to an increase of the specific volume, yet being smaller than Czero sample. The observed effect in C10 sample can be described as a negative influence of the increase of interphase thickness formed by the "*in situ*" compatibilization process. It is believed that the increasing thickness leads to a wrinkling of the interphase,[36] increasing free volume and, consequently, specific volume. Changes in free volume have been frequently associated to changes in mechanical properties of polymer blends, commonly resulting in increases of tensile strength and decreases of impact energy.[37] Despite of the tensile tests show no difference among samples, creep test was sensible enough to detect the effect of this free volume variation.

Capillary Rheometry

Figure 4 shows the apparent viscosity variation with the increasing of compatibilizer content, in different shear rates, at 250°C. It is observed that the increase of compatibilizer content increases apparent viscosity until 7 phr of compatibilizer. When the shear rate is 200 s^{-1} or less, the apparent viscosity decreases significantly with 10 phr of compatibilizer. Some authors[38–40] describe the increase in viscosity in blends reactively compatibilized. The compatibilization process generates chemical reactions between components, leading an increase of interphase interaction and, consequently, an increase in apparent viscosity. The change in the material behavior depends on the volumetric

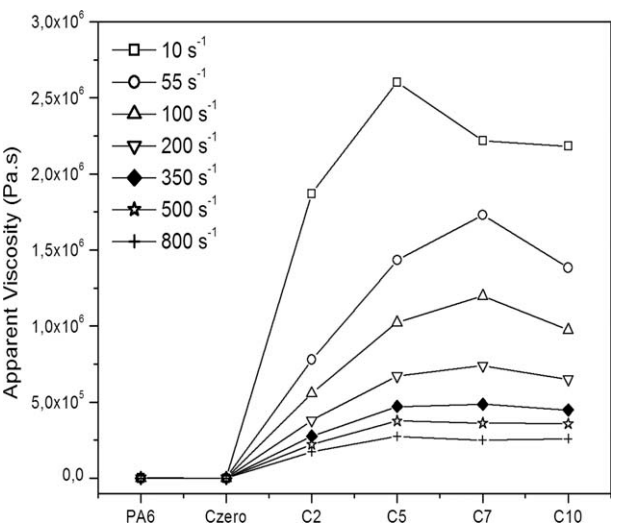

Figure 4. Shear rate scanning of samples with different compatibilizer contents, at different shear rates (the full symbol curve indicates a shear rate limit for samples behavior).

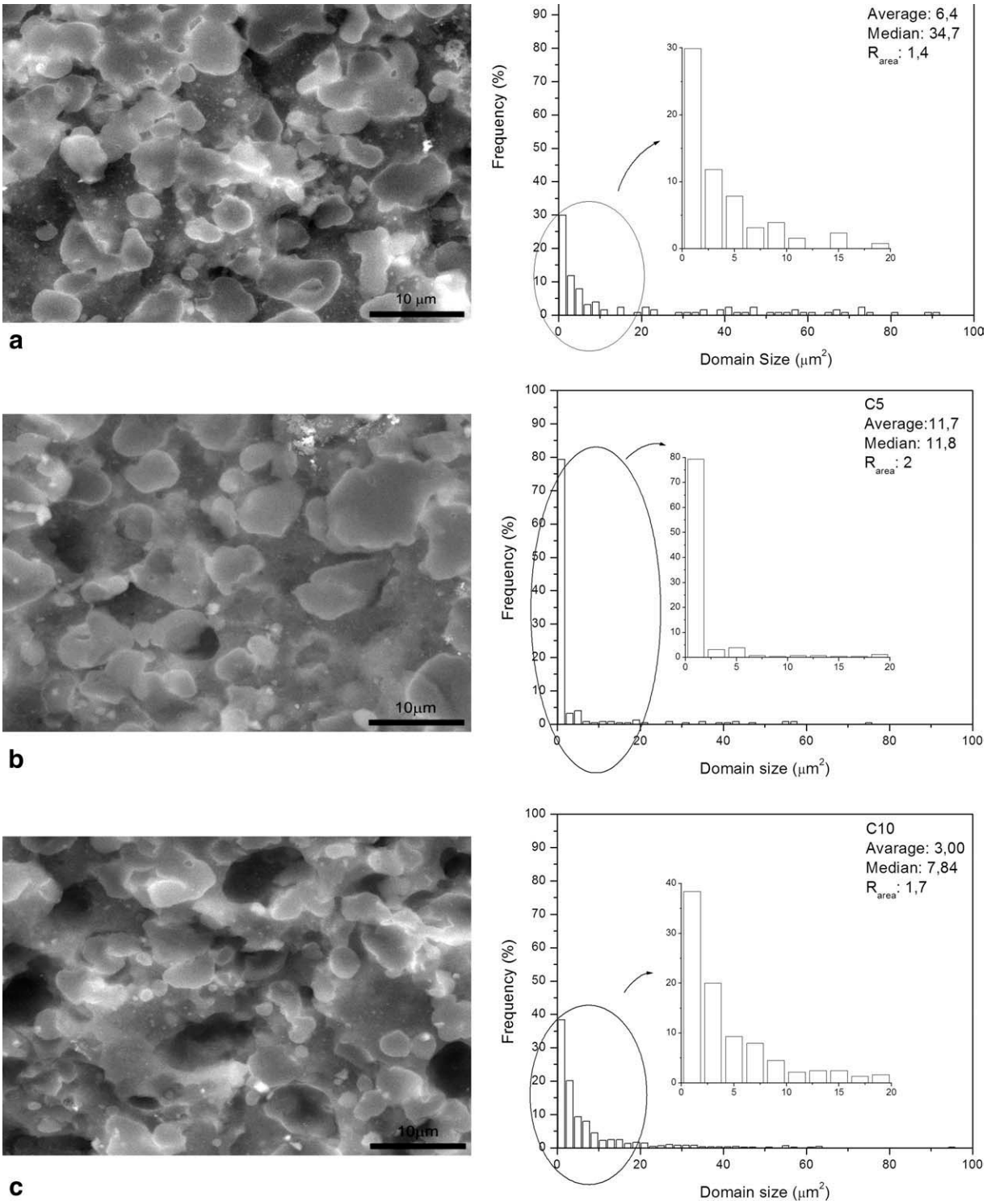

Figure 5. SEM images and domain size distribution of (a) Czero, (b) C5, and (c) C10 samples, where the brighter areas are the OsO_4 stained NBR phase, and the distribution step in all graphics correspond to 2 μm^2 of diameter.

fraction and viscoelastic properties of the interphase formed by compatibilization.[38]

Concerning to the decrease of apparent viscosity in low shear rates, for the sample with higher content of compatibilizer, George et al.[38] relates a similar behavior for PP/NBR TPVs, compatibilized with phenol-modified PP. The decrease in apparent viscosity with the increase of compatibilizer content is associated to an increase of disperse domain diameter, due to the expulsion of the compatibilizer from the interphase, generating micelles dispersed into the matrix.[36,38] This behavior can be

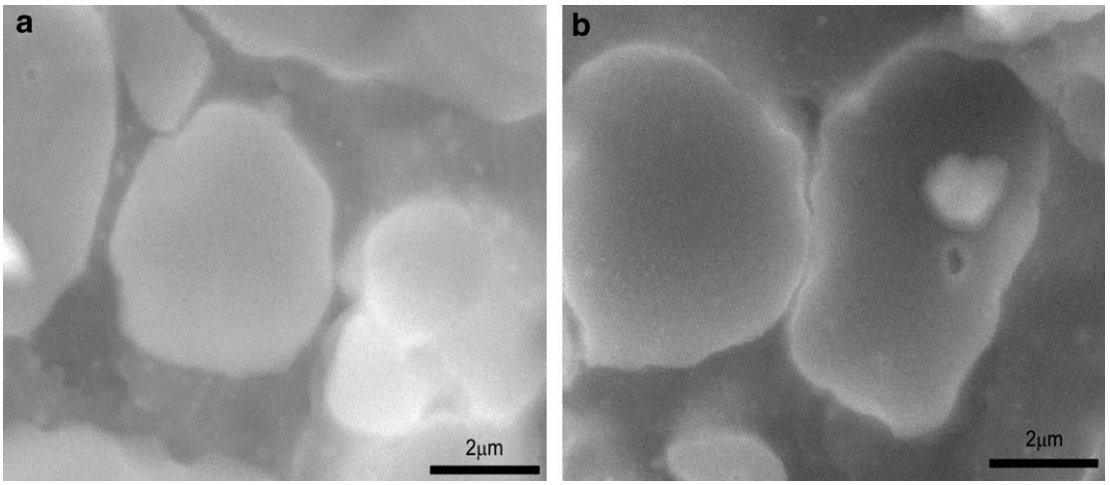

Figure 6. Higher magnitude SEM images of (a) C5 and (b) C10 samples.

observed for shear rates lower than 350 s^{-1} (limit marked by the full symbol curve). At higher shear rates, the apparent viscosity is stabilized in 5 phr of compatibilizer. The higher shear rates can be pulling out the compatibilizer from interface, normalizing the rheological behavior of the samples.

Die Swelling

The die swell is related to the elasticity of melted polymer. The elastic tendency leads the polymer molecules, once oriented by the flux into capillary tube, to try to recover its natural conformation, causing a lateral expansion of the extruded filament. It is well established that an efficient compatibilization process decreases the die swell.[38] This one decreases from 2 to 5 phr of NBR-oxa, as can be noticed in Table III. There is no change for the sample with 7 phr, and the value increases with 10 phr of compatibilizer. These results are in agreement with all results discussed so far.

Morphology

The SEM images, presented in Figure 5, show all samples with the thermoplastic phase as matrix (darker areas) and dispersed domains of elastomeric phase (brighter areas, due to osmium tetroxide staining). There are some interesting observations that must be highlighted in the images obtained. First of all, the compatibilized samples show a brighter borderline of the elastomeric phase. This effect was not observed in Czero sample. Our hypothesis consists in a stronger stain of the compatibilizer by the OsO_4, once it is more unsaturated than the NBR blend major component. It can be noticed, yet, that the sample C10 presents the brightest borderline, corroborating this hypothesis.

Other detail to be emphasized is the presence of valleys on the surface of fracture for samples Czero and C10. These valleys do not occur in the C5 sample. This fact indicates some loss of interaction between blend phases in C10 sample, with effect comparable with the no compatibilization of the blend.

Another factor that must be cited, and maybe is the most interesting detail of the image, is the presence of little brighter spots into NBR phase of C10 sample. These spots do not occur in other samples. Figure 6 shows the samples C5 and C10 in greater magnitude, for better phenomena observation. These brighter spots are supposed to be the "*in situ*" formed compatibilizer, which was expelled from the interface and, for affinity, migrated into the elastomeric phase. This hypothesis agrees with the insolubility of the "*in situ*" formed compatibilizer in acetic acid, which was confirmed by IR spectra analysis.

The Figure 5 also shows the domain size distribution of all samples. It can be noticed that the distribution is narrower than other samples. Despite of the medium domain size (D_m) do not be the smaller, it is important to notice that around 80% of the particles sized in C5 sample are between 1 and 3 μm of diameter, a frequency fairly higher than the other samples.

CONCLUSIONS

The reactive compatibilization of PA6/NBR blends leaded to significant changes in the blend morphology. Yet the tensile stress was not sensible enough to measure these changes, other characterizations were capable of indicating differences in sample behavior. The compatibilization process was efficient with 5 and 7 phr of NBR-oxa, inefficient with 2 phr, and even harmful with 10 phr of compatibilizer. The results demonstrated that the compatibilization can be evaluated by changes in creep behavior, PVT behavior, and apparent viscosity. In general, the best performance was obtained with C5 sample, once it has the best significant improvements with the lower content possible of modified polymer to be used.

ACKNOWLEDGMENTS

The authors thank CAPES, CNPq, FAPERJ, FINEP/CNPq (financial sponsoring), Petroflex, Radici, and Crompton (material supply).

REFERENCES

1. Mehrabzadeh, M.; Buford, R. P. *J. Appl. Polym. Sci.* **1996,** *64*, 1605.
2. Gessler, A. M.; Haslett, M., Jr.; William, H. *U.S. Pat.* 3,037,954, **1962.**

3. Spontak, R. J.; Patel, N. P. *Curr. Opin. Colloid. Interface Sci.* **2000,** *5*, 333.
4. Oderkerk, J.; Groeninckx, G.; Soliman, M. *Macromolecules,* **2002,** *35*, 3946.
5. Karger-Kocsis, J. Thermoplastic Rubbers via Dynamic Vulcanization. In: Shonaik, G.O.; Simon, G. P., Eds. Polymer Blends and Alloys. CRC Press: New York, **1999;** p 745.
6. Chung, O.; Coran, A. Y. *Rubber Chem. Technol.* **1997,** *70*, 781.
7. Xanthos, M. *Polym. Eng. Sci.* **1988,** *28*, 1392.
8. Koning, C.; Van Duin, M.; Pagnoulle, C.; Jerome, R. *Prog. Polym. Sci.* **1998,** *23*, 707.
9. Rodgers, B. In Rubber Compounding: Chemistry and Application; Marcel Dekker: New York; **2004,** p 569.
10. Rajesh, C.; Unnikrishnan, G.; Purushothaman, E.; Thomas, S. *J. Appl. Polym. Sci.* **2004,** *92*, 1023.
11. Piglowski, J.; Gancarz, I.; Wlazlak, M. *Polymer* **2000,** *41*, 3671.
12. Kelnar, I.; Kotek, J.; Kaprálková, L.; Hromádková, J.; Kratochvíl, J. *J. Appl. Polym. Sci.* **2006,** *100*, 1571.
13. Natov, M.; Mitova, V.; Vassieva, S. *J. Appl. Polym. Sci.* **2004,** *92*, 871.
14. Coran, A. Y.; Patel, R. *Rubber Chem. Technol.* **1981,** *54*, 91.
15. Mehrabzadeh, M.; Delfan, N. *J. Appl. Polym. Sci.* **2000,** *9*, 2057.
16. Van Dyke, J. D.; Gnatowski, M.; Burczyk, A. *J. Appl. Polym. Sci.* **2008,** *109*, 1535.
17. Bhowmick, A. K.; Inque, T. *J. Appl. Polym. Sci.* **1993,** *50*, 2055.
18. Chowdhury, R.; Banerji, M. S.; Shivakumar, K. *J. Appl. Polym. Sci.* **2007,** *104*, 372.
19. Das, P. K.; Ambatkar, S.U.; Sarma, K.S.S.; Sabharwal, S.; Banerji, M.S. *Polym. Int.* **2006,** *55*, 118.
20. Hwang, S. W.; Kim, S. W.; Park, H. Y.; Jeon, I. L.; Seo, K. H. *J. Appl. Polym. Sci.* **2011,** *119*, 3136.
21. Kumar, C. R.; Nair, S. V.; George, K. E.; Oommen, Z.; Thomas, S. *Polym. Eng. Sci.* **2003,** *43*, 1555.
22. He, C.; Zou, H.; Zhao, S. *J. Appl. Polym. Sci.* **2006,** *102*, 1374.
23. El-Nemra, K. F.; Hassana, M. M.; Alia, M. A. *Polym. Adv. Technol.* **2010,** *21*, 735.
24. Gomes, A. C. O.; Soares, B. G.; Oliveira, M. G.; Oliveira, M. F. L.; Paranhos, C. M. *e-Polym.* **2009,** n. 106.
25. Koning, C.; Van Duin, M.; Pagnoulle, C.; Jerome, R. *Prog. Polym. Sci.* **1998,** *23*, 707.
26. Almeida, M. S. M.; Guimarães, P. I. C.; Soares, B. G. *Pol.: Ciênc.Tecnol.* **2003,** *13*, 119.
27. Fornes, T. D.; Paul, D. R. *Polymer* **2003,** *44*, 3945.
28. Jeziorska, R. *Polym. Degrad. Stab.* **2005,** *90*, 224.
29. Castells, J.; Camps, F. Tables for Structural Elucidation of Organic Compounds by Spectroscopic Methods, Ed. Alhambra, Madrid; **1980,** p 56.
30. Kolarik, J.; Pefgoretti, A. *Polym. Test.* **2008,** *27*, 596.
31. Menard, K. P. Dynamic Mechanical Analysis—A Practical Introduction, 2nd ed.; CRC: New York; **1999,** Chapter 3.
32. Bicerano, J. In Prediction of Polymer Properties, 3th ed.; Marcel Dekker: New York; **2002,** Chapters 3 and 11.
33. Gomes, A. C. O.; Soares, B. G.; Oliveira, M. G.; Paranhos, C. M. *Intern. J. Polym. Anal. Charac.* **2010,** *15*, 287.
34. Fernández, M.; Munõz, M. E.; Santamaría, A. *Macromol. Chem. Phys.* **2008,** *209*, 1730.
35. Fernández, M.; Munoz, M. E.; Santamarıa, A.; Syrjala, S.; Aho, J. *J. Polym. Test.* **2009,** *28*, 109.
36. Macosko, C. W.; Jeona, H. K.; Hoye, T. R. *Prog. Polym. Sci.* **2005,** *30*, 939.
37. Hill, A. J.; Zipperz, M. D.; Tantx, M. R.; Stackx, G. M.; Jordank, T. C.; Shultz, A. R. *J. Phys. Condens. Mater.* **1996,** *8*, 3811.
38. George, S.; Ramamurthy, K.; Anand, J. S.; Groeninckx, G.; Varughese, K. T.; Thomas, S. *Polymer* **1999,** *40*, 4325.
39. Oommen, Z. ; Premalatha, C. K.; Kuriakose, B.; Thomas, S. *Polymer* **1997,** *38*, 5611.
40. Okoroafar, E. U.; Villemuire, J. P.; Agassant, J. F. *Polymer* **1992,** *33*, 5264.